Degradation Pathways and Complete Defluorination of Chlorinated Polyfluoroalkyl Substances (Cl_x−PFAS)

Jinyu Gao,[1] Zekun Liu,[1] Jun Huang,[2] and Jinyong Liu*,[1]

[1]Department of Chemical & Environmental Engineering, University of California, Riverside, California, 92521, United States

[2]State Key Joint Laboratory of Environmental Simulation and Pollution Control (SKLESPC), Beijing Key Laboratory for Emerging Organic Contaminants Control (BKLEOC), Beijing Laboratory for Environmental Frontier Technologies (BLEFT), School of Environment, Tsinghua University, Beijing 100084, China

Abstract

Chlorinated polyfluoroalkyl substances (**Cl**$_x$−PFAS) have been developed and applied for decades, but they have just been recognized as an emerging class of pollutants. This study systematically investigated the degradation of three types of **Cl**$_x$−PFAS structures, including omega-chloroperfluorocarboxylates (ω-ClPFCAs, n=1,2,4,8 **Cl**−$C_nF_{2n}COO^-$), 9-chlorohexadecafluoro-3-oxanonane-1-sulfonate (F-53B, **Cl**−$(CF_2)_6$−O−$(CF_2)_2SO_3^-$) and polychlorotrifluoroethylene oligomer acids (CTFEOAs, n=1,2,3 **Cl**−$(CF_2CF$**Cl**$)_nCF_2COO^-$) under UV/sulfite treatment. The results lead to a series of transformative insights. After initial reductive dechlorination by hydrated electron (e_{aq}^-), multiple pathways occur, including hydrogenation, sulfonation, and dimerization. In particular, this study identified the unexpected hydroxylation pathway that convert the terminal **Cl**CF_2− into $^-$OOC−, which is critical for the rapid and deep defluorination of F-53B. The hydroxylation of the middle carbons in CTFEOAs also triggers the cleavage of C−C bonds, yielding multiple −COO^- groups to promote defluorination. Hence, the Cl atoms in **Cl**$_x$−PFAS enhance defluorination in comparison with the perfluorinated analogs. After UV/sulfite treatment, the HO• oxidation of the residue leads to ~100% defluorination of all ω-ClPFCAs and CTFEOAs, without generating toxic ClO_3^- from Cl^-. This study renovates and further advances the mechanistic understanding of PFAS degradation in "advanced reduction" systems. It also suggests the synergy between "more degradable" molecular design and cost-effective degradation technology to achieve the balanced sustainability of fluorochemicals.

To effectively address the global pollution by per- and polyfluoroalkyl substances (PFAS),[1-7] it is imperative to understand the degradation mechanism and develop treatment strategies for various PFAS structures. Environmental studies on PFAS started approximately 50 years after the creation of PFAS.[8-12] Current efforts primarily focus on the "legacy" perfluorinated C_nF_{2n+1}−X (X = COO^-, SO_3^-, and $(CH_2)_m$−R, where R represents highly diverse organic moieties). Those structures have been well known as building blocks and degradation products of surfactants[13,14] and coatings.[15,16] However, "alternative" PFAS containing −O−,[17-19] –H,[20,21] and –Cl[22,23] in the fluorinated moiety (R_F) have also been systematically developed and extensively applied for decades. Recent studies have confirmed their negative health effects[24-27] and worldwide pollution in water[28-36] and soil.[37]

Chlorine-containing PFAS (**Cl**$_x$−PFAS) are prepared by the telomerization process, where the iodinated telogen (R_F−I) initiates the polymerization of fluorinated olefins (Schemes 1A and B). For enhanced stability against thermal and chemical reactions, the terminal iodine is further replaced by chlorine. The chlorination treatment costs less than fluorination (Scheme 1A).[38,39] Although the inclusion of Cl could result in higher surface tension than the perfluorinated analog,[20] the $-CF_3$ branch could yield an even lower surface tension[22] for fluoropolymer production.[40] A long-chain ether sulfonate surfactant, F-53B, contains an omega-Cl and exhibits similar surface tension to the perfluorinated (and more costly) F-53 in a wide concentration range.[41] F-53B was used as a mist suppressant for the electroplating industry in China[39] and extensively detected in the environment.[42-44] Recently, omega-chloroperfluoropolyether carboxylates (ClPFPECAs, Scheme 1C) developed for fluoropolymer synthesis[45] have been detected in the soils of densely populated New Jersey of the U.S.[37] Chlorine atoms are also included in both telogens and olefins to prepare polychlorinated PFAS.[22,38] Polychlorotrifluoroethylenes (PCTFEs, Scheme 1D) are chemically inert, nonflammable, and more cost-effective than perfluoropolyethers for the use in metal lubricants and hydraulic fluids, and have shown high haptic toxicities.[46,47] In the rat liver, PCTFEs are converted into oligomer acids (CTFEOAs), which are also chemically synthesized as commercial surfactants.[23]

Scheme 1. (A−D) Structures and Synthesis of Representative **Cl**$_x$−PFAS; (E) Previously Elucidated Degradation Pathways for ω-HPFCA as a Hydrodechlorination Product of ω-ClPFCA.

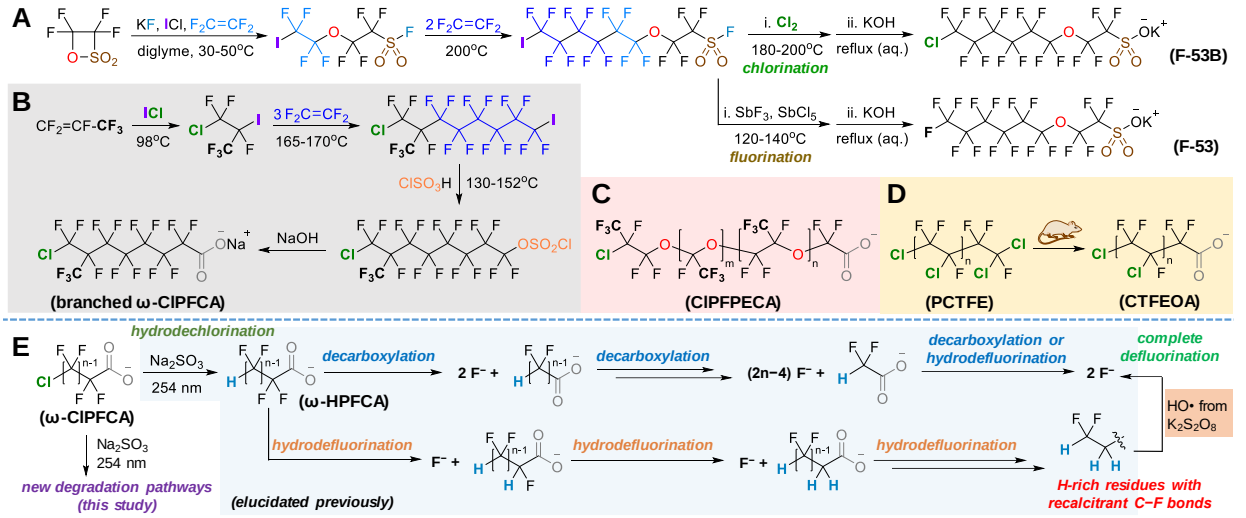

The novel structural feature and significant environmental relevance of **Cl**$_x$–PFAS require an adequate understanding of degradation mechanisms and the development of cost-effective remediation technologies. Our lab has systematically studied the transformation of legacy PFAS by UV/sulfite treatment, which produces hydrated electron (e_{aq}^-, Equation 1),[48-51] a potent species for reductive hydrodefluorination (Equations 2–3):[52,53]

$$SO_3^{2-} \rightarrow e_{aq}^- + SO_3^{-}\bullet \qquad (1)$$

$$C\text{–}F + e_{aq}^- \rightarrow C\bullet + F^- \qquad (2)$$

$$C\bullet + e_{aq}^- + H^+ \rightarrow C\text{–}H \qquad (3)$$

Based on the existing knowledge, the C–Cl bonds in **Cl**$_x$–PFAS are supposed to undergo hydrodechlorination.[54] Initially, we expected that omega-chloroperfluorocarboxylates (ω-ClPFCAs, **Cl**–$C_nF_{2n}COO^-$) would rapidly yield the omega-hydro analogs (ω-HPFCAs, H–$C_nF_{2n}COO^-$) and then degrade as previously elucidated (Scheme 1E).[55] However, our experiments with three **Cl**$_x$–PFAS families (ω-ClPFCAs, F-53B, and CTFEOAs) revealed a novel hydroxylation pathway, which reconstructs the fundamental understanding of **Cl**$_x$–PFAS degradation. This study fills major knowledge gaps towards solving the global PFAS pollution challenge: mechanistic elucidation, remediation technology, and fluorochemical design.

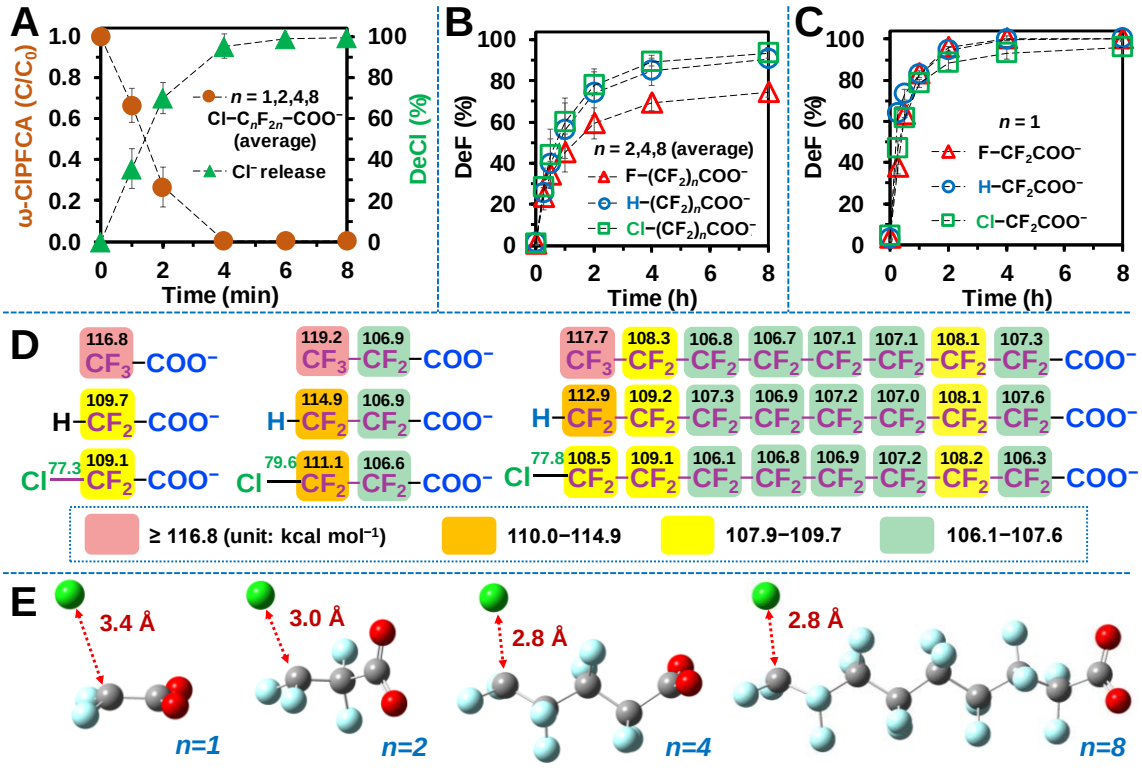

Fig. 1. Time profiles for (**A**) the degradation and dechlorination of ω-ClPFCAs and for the defluorination of (**B**) n=2,4,8 (average) and (**C**) n=1 ω-ClPFCAs, ω-HPFCAs, and PFCAs. Reaction conditions: individual PFAS (25 μM), Na_2SO_3 (10 mM), carbonate buffer (5 mM), 254 nm irradiation (18 W low-pressure Hg lamp for 600 mL of aqueous solution), pH 12.0, and 20 °C. (**D**) Calculated BDEs of C–F (in black) and C–Cl (in green) bonds of selected $[PFAS]^-$ structures and (**E**) geometry-optimized structures of $[\omega\text{-ClPFCA}]^{2-}\bullet$ at the B3LYP-D3(BJ)/6-311+G (2d,2p) level of theory.

Degradability of ω-ClPFCAs. We started with the degradation of **Cl**−$C_nF_{2n}COO^-$ (n=1, 2, 4, and 8) using the optimized reaction condition (254 nm UV, 10 mM Na_2SO_3, pH 12, see Methods and figure captions for detailed settings). The parent compound decay was completed within 8 min, accompanied by complete dechlorination (Fig.1A). The rapid Cl^- release was expected because the calculated C−Cl bond dissociation energies (BDEs, 77.3–79.6 kcal mol^{-1}) are weaker thanC−F bonds (BDE >106 kcal mol^{-1}, Fig.1D). Geometry optimization of [**Cl**–$(CF_2)_nCOO]^{2-}$•, which simulated the reaction between **Cl**–$(CF_2)_nCOO^-$ and an e_{aq}^-, resulted in spontaneous C–Cl cleavage (Fig.1E).

The defluorination percentage (deF%) of n≥2 **Cl**−$C_nF_{2n}COO^-$ reached 90−96% within 8 h (Fig.1B). Compared to the previously studied C_nF_{2n+1}−COO^- and H−$C_nF_{2n}COO^-$, **Cl**−$C_nF_{2n}COO^-$ allowed the cleavage of similar numbers of C−F bonds and left the least numbers of residual C−F bonds (Table 1). The lower deF% values from C_nF_{2n+1}−COO^- are caused by the one more C−F bond in the parent structure. The highly recalcitrant residual C−F bonds should exist in isolated fluorocarbon moieties without directly linking with $-COO^-$ (Scheme 1E). For example, CF_3−CH_2CH_2−COO^- (C−F BDE >120 kcal mol^{-1}) showed little reactivity with e_{aq}^-.[52,55,56] For n=1 structures, while the defluorination from H−CF_2COO^- and CF_3COO^- were nearly 100% within 4−8 h,[55] the defluorination from **Cl**−CF_2COO^- was up to 96% (Fig.1C). We note that the 4% disparity was not negligible. Instead, it motivated us to identify a novel reaction pathway promoted by the Cl atom.

Table 1. DeF% and Number of Cleaved and Residual F Atoms after UV/sulfite Treatment.[a]

R_F−COO^-	deF% (# of cleaved / total F atoms)[b] [# of uncleaved F atoms per molecule][b]			R_F−COO^-	deF% (# of cleaved / total F atoms)[b] [# of uncleaved F atoms per molecule][b]	
R_F	X=Cl (ω-ClPFCA)	X=H (ω-HPFCA)	X=F (PFCA)	R_F	X=Cl (CTFEOA)	X=F (PFCA)
X−CF_2− (C2)	96 ± 3.1 (1.9 ± 0.1/2F)[a] [0.1]	100 ± 1.3 (2.0 ± 0.0/2F) [0.0]	100 ± 1.0 (3.0 ± 0.0/3F) [0.0]			
X−C_2F_4− (C3)	96 ± 0.7 (3.8 ± 0.0/4F) [0.2]	90 ± 1.1 (3.6 ± 0.0/4F) [0.4]	72 ± 0.6 (3.6 ± 0.0/5F) [1.4]	**X**CF_2−CF**X**CF_2− (C4)	92 ± 4.7 (4.6 ± 0.2/5F) [0.4]	85 ± 2.1 (6.0 ± 0.2/7F) [1.0]
X−C_4F_8− (C5)	94 ± 0.4 (7.5 ± 0.0/8F) [0.5]	94 ± 4.8 (7.5 ± 0.4/8F) [0.5]	74 ± 1.0 (6.7 ± 0.1/9F) [2.3]	**X**CF_2−$(CF$**X**$CF_2)_2$− (C6)	93 ± 2.6 (7.4 ± 0.2/8F) [0.6]	89 ± 2.4 (9.8 ± 0.3/11F) [1.2]
X−C_8F_{16}− (C9)	90 ± 0.2 (14.4 ± 0.0/16F) [1.6]	88 ± 2.8 (14.1 ± 0.5/16F) [1.9]	78 ± 0.7 (13.3 ± 0.1/17F) [3.7]	**X**CF_2−$(CF$**X**$CF_2)_3$− (C8)	94 ± 3.8 (10.3 ± 0.4/11F) [0.7]	87 ± 5.8 (13.1 ± 0.9/15F) [1.9]

[a]UV/sulfite treatment conditions: PFAS (25 μM), Na_2SO_3 (10 mM), carbonate buffer (5 mM), 254 nm irradiation (18 W low-pressure Hg lamp for 600 mL of aqueous solution), pH 12.0, 20 °C, 8 h.
[b]The non-interger values are expected because of multiple degradation pathways.

Hydrochlorination Is Not the Primary Pathway. Although previous studies on UV/sulfite treatment of **Cl**−CH_2−COO^- [57] and F-53B[54] have confirmed the hydrodechlorination pathway, our transformation products (TP) analysis found novel information. After the reductive dechlorination of ω-ClPFCA (Equation 4), the omega carbon radical can be hydrogenated to yield ω-HPFCA (Fig.2A and Equation 3).

$$C–Cl + e_{aq}^- \rightarrow C\bullet + Cl^- \qquad (4)$$

However, from 25 μM of **Cl**–$C_4F_8COO^-$, the maximum concentration of H–$C_4F_8COO^-$ was merely 0.66 μM at 4 min (Fig.2B). At this time point, the rapid dechlorination of **Cl**–

$C_4F_8COO^-$ had just finished (Fig.1A), while the much slower defluorination had not proceeded to a significant level. Similarly, 25 μM of **Cl**–$C_8F_{16}COO^-$ yielded a maximum of 0.59 μM of H–$C_8F_{16}COO^-$ at 4 min (Fig.2C). For short-chain ω-ClPFCAs, we raised the initial concentration for 10-fold to facilitate the TP detection. From 250 μM of **Cl**–CF_2COO^- and **Cl**–$C_2F_4COO^-$, the maximum concentration of the corresponding products, H–CF_2COO^- and H–$C_2F_4COO^-$, were 3.7 μM at 60 min and 2.7 μM at 30 min, respectively (Figs.2D and E). Therefore, only a small fraction of the parent ω-ClPFCAs were converted to the corresponding ω-HPFCAs.

In an early study on **Cl**–CH_2COO^- degradation by UV/sulfite,[57] the radical intermediate $•CH_2COO^-$ reacted with $SO_3^{-}•$ to yield $^-O_3S–CH_2COO^-$ and dimerized to yield $^-OOCCH_2–CH_2COO^-$. Similarly, our experiments with 250 μM of **Cl**–CF_2COO^- yielded $^-O_3S–CF_2COO^-$ at the maximum concentration of 70 μM (28%) at 0.5 h (Fig.2D). Longer-chain n=2,4,8 $^-O_3S–(CF_2)_nCOO^-$ from the corresponding **Cl**–$(CF_2)_nCOO^-$ could not be quantified because analytical standards were not available. However, the high peak areas of those TPs (10^7–10^8) suggest that their abundance were not trivial. At least 19–41% of the parent **Cl**–$C_nF_{2n}–COO^-$ was converted to the dimer product $^-OOC–C_{2n}F_{4n}–COO^-$. The significant formation of sulfonated and dimerized TPs further confirms the generation of $•CF_2–(CF_2)_{n-1}COO^-$ radical upon reductive dechlorination by e_{aq}^- (Equation 4 and Fig.2A).

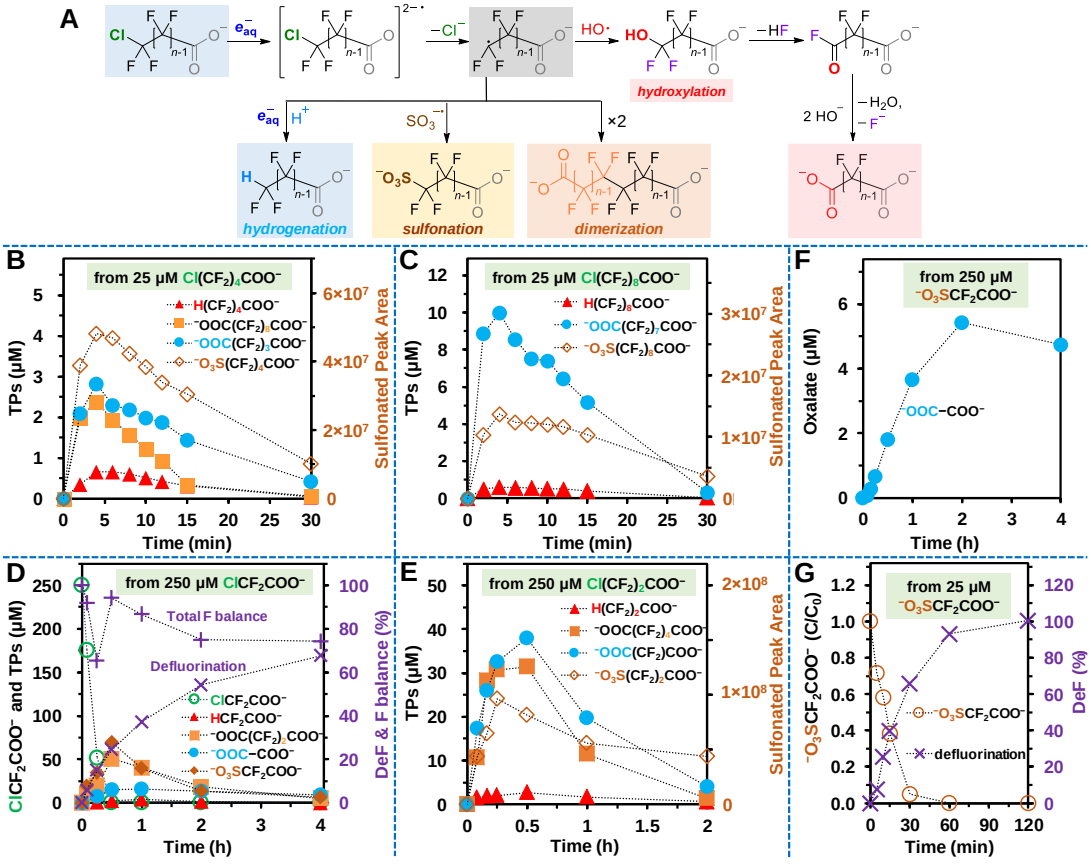

Fig. 2. (**A**) General transformation pathways after reductive dechlorination of ω-ClPFCAs; (**B**–**F**) time profiles of TPs from n=1,2,4,8 ω-ClPFCAs and $^-O_3S–CF_2–COO^-$; (**G**) degradation and defluorination of $^-O_3S–CF_2–COO^-$. Reaction conditions: individual PFAS (25 or 250 μM, as indicated), Na_2SO_3 (10 mM), carbonate buffer (5 mM), 254 nm irradiation (18 W low-pressure Hg lamp for 600 mL of aqueous solution), pH 12.0, and 20 °C.

Unexpected Hydroxylation Pathway. During the investigation of dicarboxylate TPs, we also found the unexpected $^{-}OOC-(CF_2)_{n-1}COO^{-}$, which had the same number of carbon as the parent **Cl**$-(CF_2)_nCOO^{-}$. Moreover, the maximum concentration corresponded to 11−39 % of the parent *n*=2,4,8 ω-ClPFCAs (Figs.2B, C, E). The treatment of 250 μM of **Cl**$-CF_2COO^{-}$ yielded $^{-}OOC-COO^{-}$ at the maximum concentration of 15.7 μM (6.3%) at 1 h (Fig.2D). However, UV/sulfite treatment of $H-CF_2-(CF_2)_{n-1}COO^{-}$ could not produce $^{-}OOC-(CF_2)_{n-1}COO^{-}$. Although $^{-}O_3S-(CF_2)_nCOO^{-}$ and dimeric $^{-}OOC-(CF_2)_{2n}-COO^{-}$ may produce small amounts of $^{-}OOC-(CF_2)_{n-1}COO^{-}$ via reductive C−S bond cleavage[52] and sequential decarboxylation,[53] respectively, they were not the primary source of $^{-}OOC-(CF_2)_{n-1}COO^{-}$. For example, the maximum $^{-}OOC-COO^{-}$ concentration from 250 μM of pure $^{-}O_3S-CF_2COO^{-}$ was only 5.4 μM, much less than that from 250 μM of **Cl**$-CF_2COO^{-}$. From 250 μM of pure $^{-}OOC-(CF_2)_2COO^{-}$, the formation of $^{-}OOC-COO^{-}$ (after two rounds of decarboxylation) was not detected.

Because direct oxidation of all **Cl**$_x$−PFAS with HO• resulted in negligible defluorination (Table S1), the degradation of **Cl**$_x$−PFAS required the reaction with e_{aq}^{-}. We propose that after reductive dechlorination of **Cl**$-(CF_2)_nCOO^{-}$, the $\bullet CF_2-(CF_2)_{n-1}COO^{-}$ intermediate could react with a HO• to yield unstable perfluorinated alcohol,[58] which spontaneously evolves into $^{-}OOC-(CF_2)_{n-1}COO^{-}$ (Fig.2A). Further degradation of such TPs was also confirmed (Tables S2 and S3). Because HO• is present in UV/sulfite system,[59,60] we added methanol to scavenge HO•.[61] As expected, the yield of $^{-}OOC-(CF_2)_{n-1}COO^{-}$ was lowered, and the production of $H-(CF_2)_nCOO^{-}$ was increased (Fig.S1). However, the overall deF% from **Cl**$-(CF_2)_nCOO^{-}$ were not impacted because (i) methanol is not a significant scavenger of e_{aq}^{-} and (ii) ω-HPFCAs and perfluorodicarboxylates (PFdiCAs) allowed the same number of C−F bonds to be cleaved by UV/sulfite treatment.[55] The reactivity of $^{-}O_3S-(CF_2)_nCOO^{-}$ is assumed to be similar to $H-(CF_2)_nCOO^{-}$ or $F-(CF_2)_nCOO^{-}$.

Mass Balance Analysis. Because most TPs from **Cl**$-CF_2COO^{-}$ are quantifiable with standard chemicals and the *n*=1 structure limited the number of reaction sites, we were able to close 94% of the total F balance at 30 min (Fig.2D). This value is the highest F mass balance we have ever achieved from UV/sulfite treatment of PFAS. Therefore, we propose that the four pathways (hydrogenation, sulfonation, dimerization, and hydroxylation) could represent the major degradation pathways upon the dechlorination by e_{aq}^{-}. Both $^{-}O_3S-CF_2COO^{-}$ (Fig.2G) and $H-CF_2COO^{-}$ allowed 100% defluorination by UV/sulfite treatment, whereas $^{-}OOC-(CF_2)_2COO^{-}$ allowed up to 83% defluorination.[55] Therefore, the incomplete defluorination (96%, Fig.1C) of **Cl**$-CF_2COO^{-}$ can be attributed, at least partially, to the dimerization pathway. More importantly, the experimental results have shown that (i) the previously reported hydrodechlorination is the least preferred reaction pathway among the four and (ii) oxidative species such as HO• are playing significant roles in the UV/sulfite system. However, detailed mechanistic eludication for the oxidative species warrants further studies. A complete set of degradation pathways for long-chain and perfluorinated structures remain largely unknown. Our lab is investigating that aspect and will report the findings in the near future.

New Mechanistic Insights into F-53B Degradation. Similar to ω-ClPFCAs, the ether sulfonate F-53B exhibited rapid and complete dechlorination within 6 min (Fig.3A) and 73% defluorination at 12 h (Fig.3B). The trend of calculated C−F and C−Cl BDEs (Fig.3G) in F-53B versus its hydro- and perfluorinated analogs is similar to the all-carbon-chain structures (Fig.1D). The spontaneous C−Cl cleavage from $[\mathbf{Cl}-(CF_2)_6O(CF_2)_2SO_3]^{2-}\bullet$ (Fig.3G) supports the reductive dechlorination mechanism. Like ω-ClPFCA, F-53B yielded $H-(CF_2)_6O(CF_2)_2SO_3^{-}$ (structure **a** in

Fig.3H), $^{-}O_3S-(CF_2)_6O(CF_2)_2SO_3^{-}$ (**b**), and $^{-}OOC-(CF_2)_5O(CF_2)_2SO_3^{-}$ (**c**) (Fig.3C). The dimerized structure exceeded the molecular weight limit we set for suspect TP detection. A series of shorter-chain TPs, $^{-}OOC-(CF_2)_nO(CF_2)_2SO_3^{-}$ (n=4,3,2,1, structures **d**–**g** in Fig.3H), showed decreasing abundance as the $-(CF_2)_n-$ moiety became shorter (Fig.3D). Because we did not detect any shorter-chain F-53B analog impurities (i.e., n=1–5 **Cl**$-(CF_2)_nO(CF_2)_2SO_3^{-}$) in the t=0 sample, the shorter-chain $^{-}OOC-(CF_2)_nO(CF_2)_2SO_3^{-}$ TPs **d**–**g** most probably came from the stepwise decarboxylation[52] from **c** (Fig.3H). Notably, all carboxylate TPs became non-detectable after 4 h (Fig.3D), whereas significant defluorination continued to 8 h (Fig.3B).

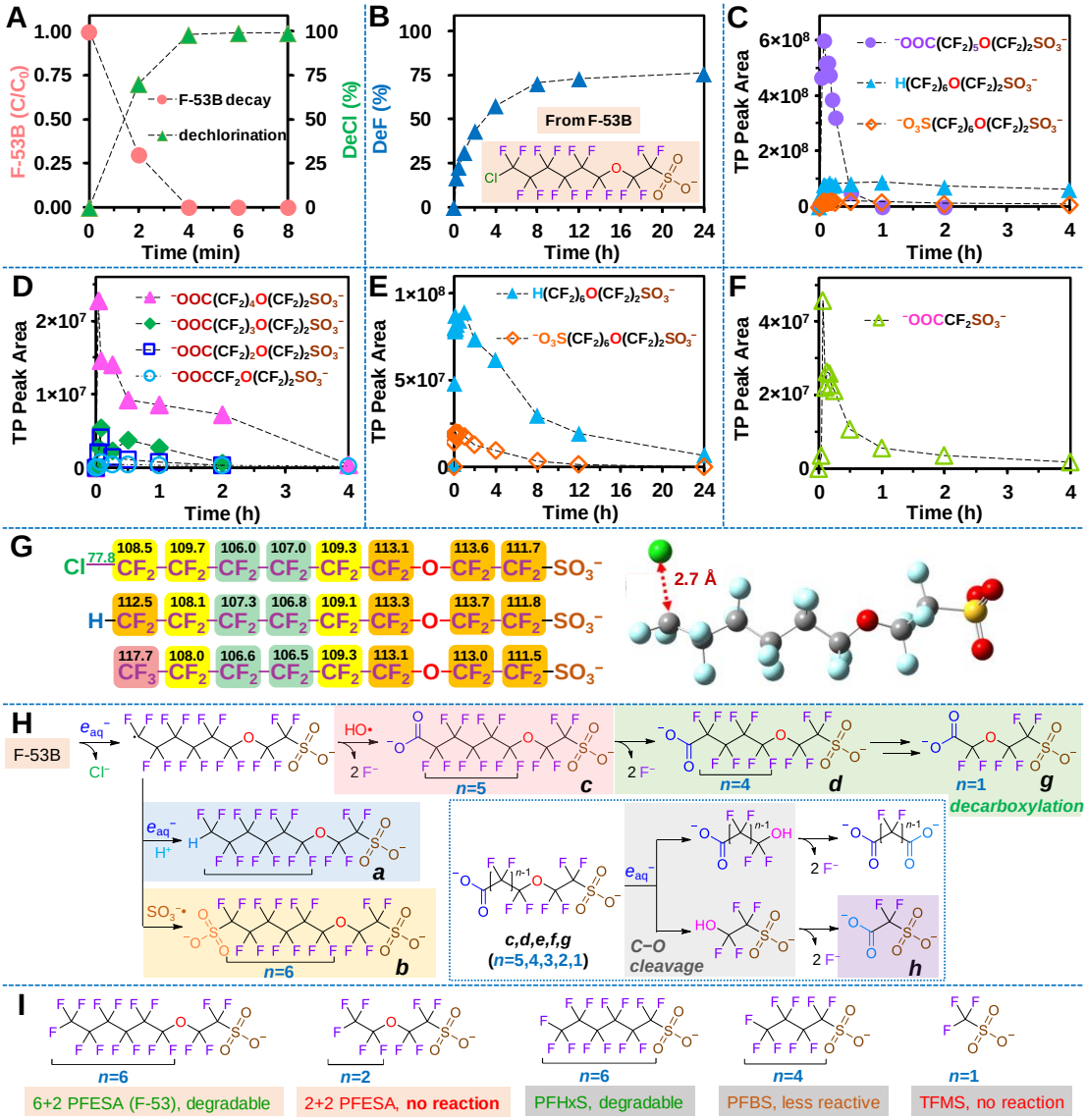

Fig. 3. Time profiles of (**A**) parent structure decay and dechlorination, (**B**) defluorination, and (**C**–**F**) transformation products of F-53B. Reaction conditions: F-53B (25 μM), Na_2SO_3 (10 mM), carbonate buffer (5 mM), 254 nm irradiation (18 W low-pressure Hg lamp for 600 mL of aqueous solution), pH 12.0, and 20 °C. (**G**) Calculated BDEs of C–F and C–Cl of F-53B and structure analogs and the geometry-optimized structure of $[\mathbf{Cl}-(CF_2)_6O(CF_2)_2SO_3]^{2-}\bullet$ at the B3LYP-D3(BJ)/6-311+G (2d,2p) level of theory. (**H**) Proposed reaction scheme. HRMS-detected TPs are assigned with letters. (**I**) Reactivity comparison with other perfluorinated sulfonate structures.

In comparison to **c**−**g**, the hydrogenated TP **a** and sulfonated TP **b** degraded much slower (Fig.3E). A previous study proposed that the reaction between **a** and e_{aq}^- triggered C−O cleavage.[54] However, our experimental results led to a different interpretation. First, if C−O cleavage occurred in **a**, the short moiety $\bullet(CF_2)_2SO_3^-$ (or $\bullet O(CF_2)_2SO_3^-$) would evolve into $^-OOC{-}CF_2SO_3^-$ (**h**) via the unstable $HO(CF_2)_2SO_3^-$.[62] Although **h** was detected as a significant TP (Fig.3F), its abundance became negligible after 4 h, when a major fraction of **a** still remained (Fig.3E). Thus, the formation of **h** from **a** is less likely.

Second, although spontaneous C−O cleavage has been confirmed from the reaction between perfluoroether carboxylates (PFECAs) and e_{aq}^-,[62] we wondered whether this mechanism applies to perfluoroether sulfonates (PFESAs). Thus, we tested a short-chain model, $CF_3CF_2{-}O{-}(CF_2)_2{-}SO_3^-$. To our surprise, this C2+C2 PFESA did not show any decay or defluorination. This result differs entirely from short-chain PFECAs that exhibited rapid decay and significant defluorination.[62] Apparently, the C−O cleavage mechanism does not readily occur for PFESA. Moreover, the previous study on F-53B degradation also reported complete decay and significant defluorination of F-53 (perfluorinated $F{-}(CF_2)_6O(CF_2)_2SO_3^-$, not available for this study).[54] The relatively facile degradation of C6+C2 PFESA and no reactivity of C2+C2 PFESA resemble the comparison among n=6, 4, and 1 $C_nF_{2n+1}{-}SO_3^-$.[52,56] Lacking a terminal $-COO^-$, the reactivity of perfluoroalkane sulfonates strongly depends on the fluoroalkyl chain length. PFBS was substantially more recalcitrant than PFOS, and TFMS did not show any degradation (Fig. 3I).

Third, our previous study on PFECAs has confirmed that C–O cleavage occurred regardless of how many $-CF_2-$ units separate the ether bond and terminal $-COO^-$.[62] Therefore, the $^-OOC{-}(CF_2)_nO(CF_2)_2SO_3^-$ are the most probable TPs that allow reductive C–O cleavage and thus produce **h** as the common TP (Fig.3H). Notably, **h** allowed 100% defluorination (Fig.2G) as compared with no degradation of $CF_3{-}SO_3^-$. Therefore, the above results reconstruct the mechanistic insights into F-53B degradation. The previously unexpected hydroxylation TPs **c**−**g** allow favorable defluorination mechanisms (i.e., decarboxylation and C–O cleavage) and thus a deep defluorination (Fig.3B).

C−C Bond Cleavage Identified from CTFEOA Degradation. The three CTFEOAs (n=1, 2, 3 $\mathbf{Cl}{-}(CF_2CF\mathbf{Cl})_nCF_2COO^-$) underwent rapid decay within 2−4 min (Figs.4A,C,E). Because each structure contains multiple C−Cl bonds, the complete dechlorination took longer than the parent compound decay. Calculations found that C−Cl bonds on the secondary carbons (−CF**Cl**−; 65.2−71.9 kcal mol^{-1}, Fig.4G) are weaker than those on the primary carbons (**Cl**CF_2−; 75.7−76.1 kcal mol^{-1}). The spontaneous C−Cl bond cleavage upon adding one extra electron (i.e., $[\mathbf{Cl}(CF_2CF\mathbf{Cl})_nCF_2COO]^{2-}\bullet$) occurred on the second carbon counted from the terminal $\mathbf{Cl}F_2C{-}$ (Fig.4H). The overall deF% from CTFEOAs (92−94%) were higher than PFCAs ($C_nF_{2n+1}{-}COO^-$) containing the same number of carbon (85−88%, Figs.4B,D,F). In particular, the defluorination from CTFEOAs in the first 15 min was much deeper than PFCAs. The difference is more significant for longer CTFEOAs, which contain more C−Cl bonds. The numbers of residual C−F bonds in CTFEOAs after treatment were lower than those in PFCAs (Table 1). Moreover, CTFEOAs reached the maximum deF% within 4 h, half of the time needed for PFCAs (Figs.4B,D,F).

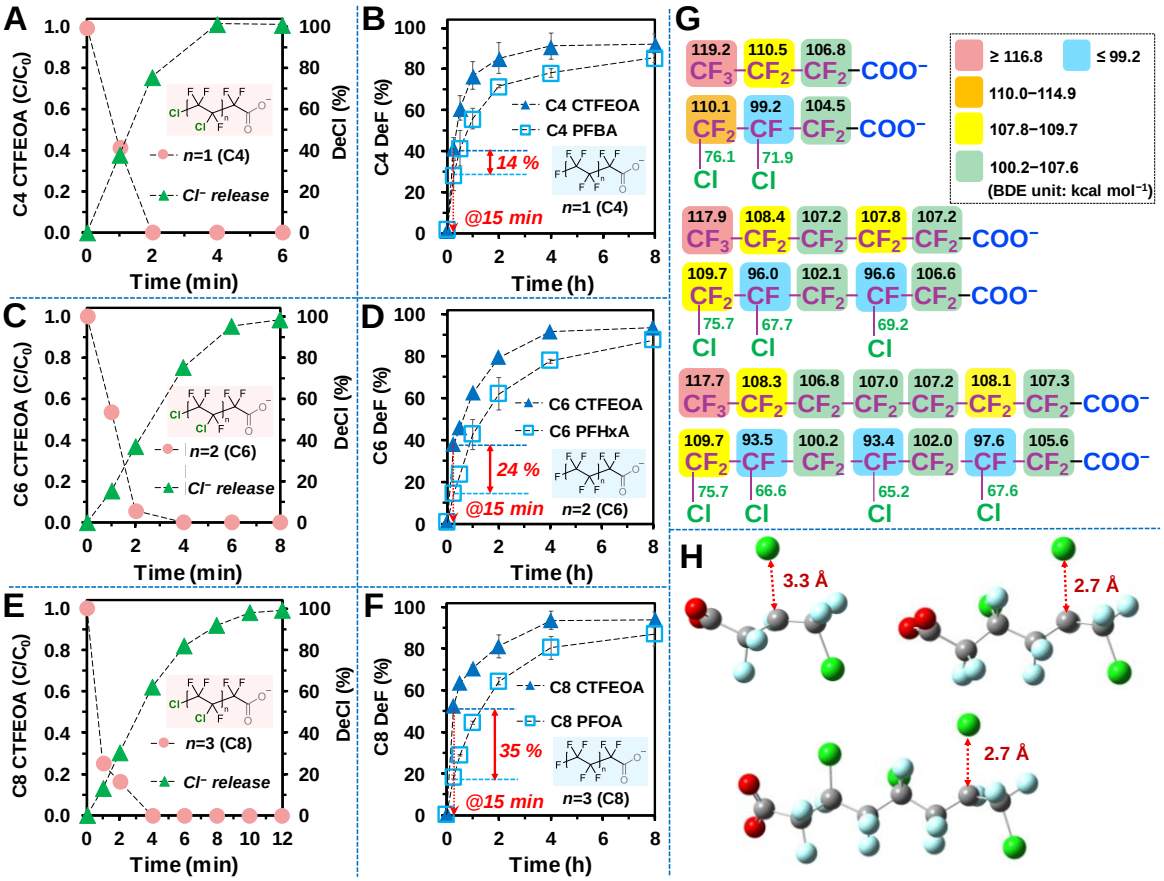

Fig. 4. Time profiles of parent structure decay and dechlorination (**A,C,E**) and defluorination (**B,D,F**) of the three CTFEOAs. The defluorination of the three PFCAs in the same chain lengths are compared, with the indicated difference at 15 min. Reaction conditions: CTFEOA or PFCA (25 μM), Na_2SO_3 (10 mM), carbonate buffer (5 mM), 254 nm irradiation (18 W low-pressure Hg lamp for 600 mL of aqueous solution), pH 12.0, and 20 °C. (**G**) Calculated BDEs of C−F and C−Cl of $[CTFEOA]^-$ and $[PFCA]^-$ structures and (**H**) geometry-optimized structures of $[CTFEOA]^{2-}$• at the B3LYP-D3(BJ)/6-311+G (2d,2p) level of theory.

The hydroxylation mechanism is also evidenced by CTFEOA degradation. We observed rapid formation of C3 $^-OOC{-}CF_2{-}COO^-$ from all three CTFEOAs (Figs.5A–C). The C5 TP, $^-OOC{-}CF_2CF\mathbf{Cl}{-}CF_2{-}COO^-$, was also produced from both C6 and C8 parents. The chain-shortened TPs indicate C–C bond cleavage. Upon dechlorination, the hydroxylated carbon is converted into $-COO^-$ accompanied by the C–C bond cleavage, probably in a homolytic pattern (Fig.5D). Although detailed mechanisms remain elusive and warrant further investigation, similar phenomenon was reported in a patent in 1961, where the hydrolysis of $C_4F_9{-}CF(OSO_2Cl){-}CF_3$ yielded $C_4F_9{-}COO^-$ (Fig.5E).[38] More importantly, the C3 $^-OOC{-}CF_2{-}COO^-$ from C4 CTFEOA and C5 $^-OOC{-}CF_2CF\mathbf{Cl}{-}CF_2{-}COO^-$ from C6 CTFEOA evidence that the dominating reductive dechlorination occurred on the relatively weak C–Cl bond (Figs.4G and H). The remaining C–Cl in the C5 TP can be further cleaved to yield C3 $^-OOC{-}CF_2{-}COO^-$ (Fig.5D).

Multiple mono-sulfonated TPs (i.e., with one −Cl replaced by $-SO_3^-$) were also identified, each with a different retention time in the HPLC column (Fig.S2), indicating that all C–Cl bonds can be reductively cleaved and the carbon radicals can react with SO_3^-• (or other radical species).

A double hydrogenated product was observed from C4 CTFEOA (Fig.5A), but the attempts to identify all possible H/Cl exchanged TPs from C6 and C8 CTFEOAs were not successful. This is probably because the diverse substitutions (e.g., H^++e_{aq}^-, SO_3^-•, and HO•) upon dechlorination at multiple carbons significantly lowered the abundance of individual TPs. Despite of the complex reaction pathway network, we prioritized the focus on filling the remaining 6−8% gap from the goal of complete defluorination of most **Cl$_x$**−PFAS structures.

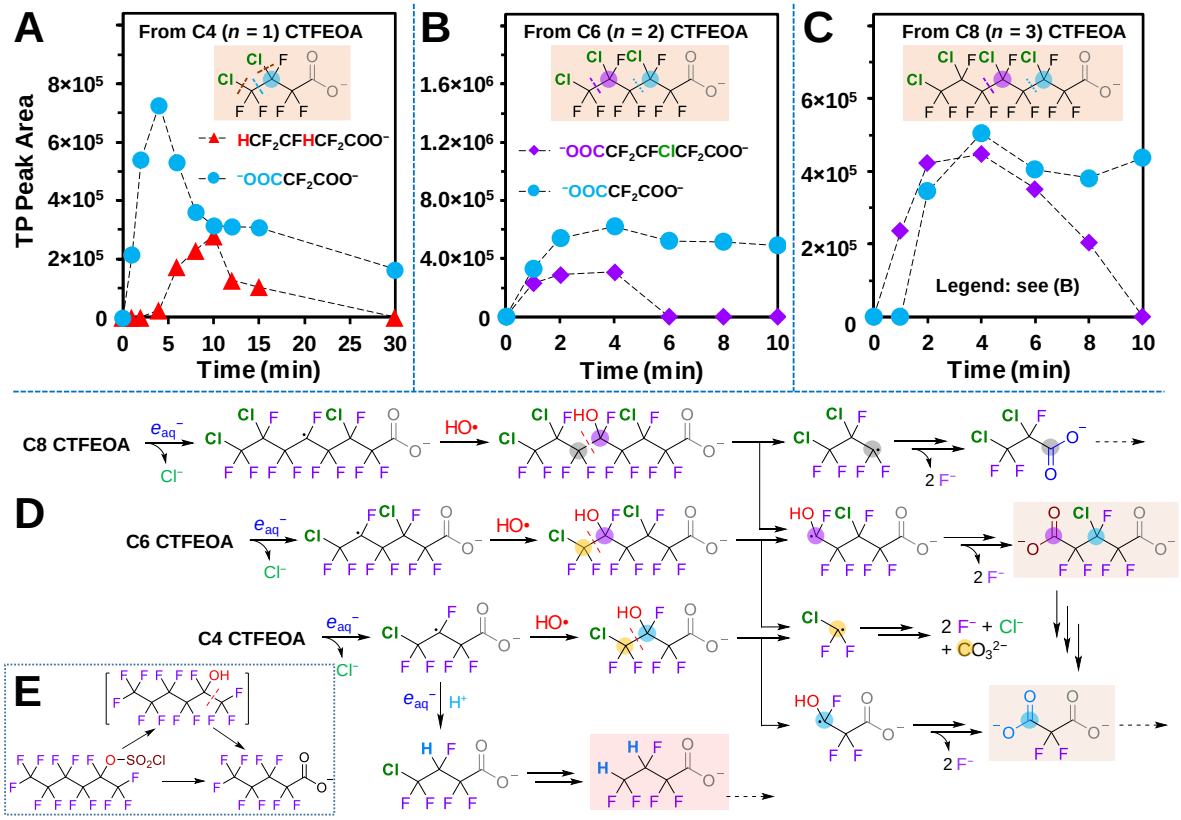

Fig. 5. (**A**−**C**) Time profiles of TPs from the three CTFEOAs in the beginning of reactions, (D) proposed reaction mechanisms and pathways, and (E) a reported reaction for mechanistic comparison. The carbon atoms involved in characteristic C−C bond cleavage were highlited with colors. Reaction conditions: CTFEOA (25 μM), Na_2SO_3 (10 mM), carbonate buffer (5 mM), 254 nm irradiation (18 W low-pressure Hg lamp for 600 mL of aqueous solution), pH 12.0, and 20 °C.

Further Defluorination of Cl$_x$−PFAS by the Following Oxidation. The sequential treatment using UV/sulfite followed by heat/persulfate has allowed near-complete defluorination from most PFCAs and PFSAs.[56] After the UV/sulfite treatment, residues containing C−H bonds allow extensive oxidation so that the isolated CF_3− or −CF_2− can be hydroxylated and thus defluorinated. As expected, both SO_4^-• (initial pH=2) and HO• (initial pH>12) were capable of cleaving residual C−F bonds and resulted in 99−103% overall deF% of all four ω-ClPFCAs and three CTFEOAs (Table 2, entries 1−7). The exception is F-53B (entry 8), where the following oxidation brought deF% from 76% (after UV/sulfite for 24 h) to 93%. We attribute the incomplete defluorination to recalcitrant structures containing long fluoroalkyls, such as H−$(CF_2)_6O(CF_2)_2SO_3^-$, which remained in a significant abundance at 24 h (Figs.3E and H). Oxidation using either SO_4^-• or HO• could only trigger very limited defluorination from oxidizing the terminal C−H bond.[55]

We further examined the potential formation of the toxic byproduct chlorate (ClO_3^-)[63,64] from Cl^-, both a ubiquitous water component and the **Cl$_x$**−PFAS dechlorination product. The SO_4^-• treatment of **Cl$_x$**−PFAS defluorination residues oxidized a small portion of Cl^- into ClO_3^- (Table 2). In the absence of organic residues from **Cl$_x$**−PFAS defluorination, the yield of ClO_3^- from the same concentration of Cl^- was elevated (entry 9 versus entries 1−4, and 8). In sharp contrast, the use of HO• in all cases produced negligible ClO_3^-, if any (lower than the detection limit).

Table 2. Defluorination and Chlorate Formation by Oxidative Treatment.[a]

entry	UV/sulfite residue[b] or NaCl solution	[Cl^-] (μM)	oxidation with HO•		oxidation with SO_4^-•	
			deF%	ClO_3^- (μM)	deF%	ClO_3^- (μM)
1	**Cl**−CF_2−COO^-	25	101 ± 0.5	< 0.1[c]	101 ± 0.2	0.7 ± 0.1
2	**Cl**−C_2F_4−COO^-	25	100 ± 0.7	< 0.1	101 ± 1.6	0.5 ± 0.1
3	**Cl**−C_4F_8−COO^-	25	103 ± 1.7	< 0.1	103 ± 2.2	0.5 ± 0.1
4	**Cl**−C_8F_{16}−COO^-	25	99 ± 0.5	< 0.1	100 ± 1.4	0.4 ± 0.1
5	**Cl**CF_2−CF**Cl**CF_2−COO^-	50	100 ± 1.5	< 0.1	100 ± 0.9	1.4 ± 0.4
6	**Cl**CF_2−$(CF$**Cl**$CF_2)_2$−COO^-	75	102 ± 0.7	< 0.1	103 ± 2.0	2.2 ± 0.2
7	**Cl**CF_2−$(CF$**Cl**$CF_2)_3$−COO^-	100	103 ± 1.0	< 0.1	101 ± 0.3	3.0 ± 0.1
8	**Cl**C_6F_{12}−O−C_2F_4−SO_3^-	25	93	< 0.1	94	0.4
9	25 μM NaCl	25	-	< 0.1	-	1.4 ± 0.1
10	500 μM NaCl	500	-	< 0.1	-	143.6 ± 6.3

[a]Oxidative post-treatment conditions: $K_2S_2O_8$ (5 mM), initial pH adjusted to 12.3 by NaOH for the dominance of HO• or adjusted to 2.0 by H_2SO_4 for the dominance of SO_4^-•, 120 °C, 40 min.
[b]UV/sulfite treatment conditions: PFAS (25 μM), Na_2SO_3 (10 mM), carbonate buffer (5 mM), 254 nm irradiation (18 W low-pressure Hg lamp for 600 mL of aqueous solution), pH 12.0, and 20 °C, 8 h (for ω-ClPFCAs and CTFEOAs) or 24 h (for F-53B).
[c]The detection limit by ion chromatography is 0.1 μM.

Implications for Environmental Remediation. Early patents on numerous **Cl$_x$**−PFAS products for various applications and recent reports on worldwide detection of diverse **Cl$_x$**−PFAS pollutants suggest broad impacts of this "old but novel" chloro-fluoro-chemical family. Our experimental results evidence a hydroxylation pathway upon reductive dechlorination by e_{aq}^-. This unexpected mechanism outweighs the existing knowledge of hydrodechlorination and is highly beneficial to environmental remediation. First, hydroxylation of a fluorinated carbon triggers spontaneous conversion into a $-COO^-$ (Figs.2A, 3H, and 5D). Perfluorinated carboxylates have the highest degradability among all reported PFAS pollutants.[52,56] Second, a C−Cl bond integrated into sulfonate-terminal PFAS will substantially enhance the degradability by introducing $-COO^-$. This feature is particularly important for degrading non-carboxylate short-chain structures (Fig.2G versus 3I). Third, the reductive C−O cleavage pathway, which is critical for deep defluorination of ether structures, is exclusive for carboxylates (Fig.3H). Fourth, the comparison of defluorination kinetics for CTFEOAs versus PFCAs (Table 1 and Figs.4B, D, F) suggests that the inclusion of multiple C−Cl bonds can reduce the UV energy consumption by at least 50%. In addition, even if a small portion of C−Cl bonds were converted into C−H bonds, our previous study has shown that ω-HPFCAs favor the desirable decarboxylation pathway for defluorination over PFCAs.[55]

Implications for PFAS Chemical Design. In the real world, PFAS chemicals cannot be immediately phased out from all fields due to their unique properties for a broad scope of applications.[65] The fluorine-free replacements could even result in a higher toxicity.[66] For the future design, manufacturing, and management of specialty PFAS products, it would be imperative to enhance the degradability without sacrificing the desirable property. The inclusion of one or more Cl atoms in the PFAS structure could be a potential solution. Earlier works have demonstrated that the negative impact of replacing a F atom with a Cl atom on surfactant properties

can be offset by flexible molecular designs.[22,41] This proof-of-concept study also verifies that the use of 254 nm UV, sulfite, hydroxide, and persulfate (or other common chemicals and approaches producing HO•), all of which are essential components of practical water and wastewater treatment,[67] can achieve near 100% defluorination of various **Cl$_x$**−PFAS with minimized formation of toxic byproducts. This study has thus demonstrated, from the perspective of chemistry, that the synergy of environmental-friendly PFAS design and cost-effective PFAS degradation technologies can achieve the balanced environmental sustainability of fluorochemicals.

Methods.

Chemicals. ω-ClPFCAs (**Cl**−C_nF_{2n}−COOH; n=1,2,4,8), CTFEOAs (**Cl**−(CF_2CF**Cl**)$_n$−CF_2−COOH; n=1,2,3), F-53B (**Cl**−C_6F_{12}−O−C_2F_4−SO_3K), perfluoro(2-ethoxyethane)sulfonic acid (C_2F_5−O−C_2F_4−SO_3H), and 2-(fluorosulfonyl)difluoroacetic acid (FO_2S−CF_2−COOH) were obtained in bulk quantities (i.e., 0.1–5 g) and used as received. All acids were prepared into 10 mM stock solutions by mixing with excess NaOH (20 mM) for deprotonation. The solution of 25 μM FO_2S−CF_2−COOH was hydrolyzed into ^-O_3S−CF_2−COO^- at 20 °C and pH 12 overnight.[68] The information on CAS numbers, purities, and vendors are listed in the Supplementary Information (SI). Sodium sulfite (Na_2SO_3), sodium bicarbonate ($NaHCO_3$), sodium hydroxide (NaOH), potassium persulfate ($K_2S_2O_8$), and sulfuric acid (H_2SO_4) were purchased from Fisher Chemical.

UV/sulfite Treatment. The reactor configuration[52,53,56] and photochemical parameters[69] have been established in our previous studies. Briefly, a 600 mL aqueous solution containing 25 μM individual PFAS, 5 mM $NaHCO_3$, and 10 mM Na_2SO_3 was loaded into the photoreactor (assembled with Ace Glass parts #7864-10, #7874-38, and #7506-14, and wrapped with aluminum foil). The solution was irradiated by an 18 W low-pressure mercury lamp (GPH212T5L/HO) placed in the quartz immerse well. The temperature was maintained at 20 °C by the jacketed cooling water. Prior to the reaction, N_2 sparging was not needed[52] because the initially dissolved oxygen (up to 0.25 mM at the saturated level at room temperature) was readily depleted by sulfite.[70] All three outlets of the photoreactor were sealed with rubber stoppers to prevent air intrusion.

Subsequent Oxidation by Heat/persulfate. After UV/sulfite treatment, the 30 mL aliquots of the resulting solution were amended with 5 mM $K_2S_2O_8$ and added with either H_2SO_4 to pH 2.0 or with 12.5 mM NaOH to pH ~12.4. The solutions were loaded in glass reaction tubes and heated at 120 °C for 40 min in a pressure cooker (Farberware 6 Quart).[56] Thermal decomposition of $S_2O_8^{2-}$ yielded two equivalents of sulfate radical (SO_4^-•). The SO_4^-• is preserved at pH 2.0 or fully converted into a hydroxyl radical (HO•) at pH>12.[71] Since the 1960s, thermal digestion of environmental samples using $S_2O_8^{2-}$ has been extensively adopted[72-74] due to its high efficiency in mineralizing organic structures. Our proof-of-concept studies have used this approach to probe the "upper limit" of oxidative conversion of PFAS.[55,56]

Sample Analyses. Fluoride ion (F^-) release was measured by a Fisherbrand accumet solid-state ion-selective electrode connected to a Thermo Scientific Orion Versa Star Pro meter. This method has been validated by ion chromatography (IC)[52] and solution matrix spiking tests.[56] Chloride ion (Cl^-) release was measured by IC. The percentages of defluorination (deF%) and dechlorination (deCl%) are defined as the ratios between released F^-/Cl^- and total F/Cl in the parent **Cl$_x$**−PFAS. A liquid chromatography high-resolution mass spectrometer (LC-HRMS) was used to (i) quantify parent PFAS and transformation products (TPs) that have pure chemicals as

the analytical standards and (ii) screen TPs without analytical standards. Very short-chain PFAS, including chlorodifluoroacetate (**Cl**−CF_2COO^-), difluoroacetate (H−CF_2COO^-), and oxalate ($^-$OOC−COO^-), were quantified by IC. Detailed operation conditions and procedures for IC and LC-HRMS are described in the SI.

Theoretical Calculations. Density functional theory (DFT) calculations on C–F and C–Cl bond dissociation energies (BDEs) in the deprotonated [**Cl**$_x$−PFAS]$^-$ and the optimized structure with an added e_{aq}^- (i.e., [**Cl**$_x$−PFAS]$^{2-}$•) followed our previous approach.[52,62,75] Results from these approaches have been consistent with those from condensed Fukui Function in terms of predicting the site of reductive PFAS transformation.[55]

Acknowledgment

Financial support was provided by the Strategic Environmental Research and Development Program (ER18-1289 and ER20-1541) and the National Science Foundation (CHE-1709719). Dr. Siwen Wang provided background information and help discussion on F-53B.

Supplemental Information

Detailed information on PFAS chemicals; measurement of parent PFAS, transformation products, chloride, and chlorate; defluorination from the direct oxidation of **Cl**$_x$−PFAS with HO•; the effect of methanol on TPs; the formation of sulfonated products from CTFEOAs.

Author Information

Corresponding Author *(J.L.) E-mail: jinyongl@ucr.edu; jinyong.liu101@gmail.com.

The authors declare no competing financial interest.

References

1 Key, B. D., Howell, R. D. & Criddle, C. S. Fluorinated organics in the biosphere. *Environ. Sci. Technol.* **31**, 2445-2454 (1997).
2 Moody, C. A. & Field, J. A. Perfluorinated surfactants and the environmental implications of their use in fire-fighting foams. *Environ. Sci. Technol.* **34**, 3864-3870 (2000).
3 Wang, Z., DeWitt, J. C., Higgins, C. P. & Cousins, I. T. A never-ending story of per-and polyfluoroalkyl substances (PFASs)? *Environ. Sci. Technol.* **51**, 2508-2518 (2017).
4 Lohmann, R. *et al.* Are fluoropolymers really of low concern for human and environmental health and separate from other PFAS? *Environ. Sci. Technol.* **54**, 12820-12828 (2020).
5 Kwiatkowski, C. F. *et al.* Scientific basis for managing PFAS as a chemical class. *Environ. Sci. Technol. Lett.* **7**, 532-543 (2020).
6 Ng, C. *et al.* Addressing urgent questions for PFAS in the 21st century. *Environ. Sci. Technol.* **55**, 12755-12765 (2021).
7 Lau, C., Butenhoff, J. L. & Rogers, J. M. The developmental toxicity of perfluoroalkyl acids and their derivatives. *Toxicol. Appl. Pharmacol.* **198**, 231-241 (2004).
8 Simons, J. H. & Block, L. Fluorocarbons. The reaction of fluorine with carbon. *J. Am. Chem. Soc.* **61**, 2962-2966 (1939).
9 Hanford, W. & Joyce, R. Polytetrafluoroethylene. *J. Am. Chem. Soc.* **68**, 2082-2085 (1946).
10 Kauck, E. A. & Diesslin, A. R. Some properties of perfluorocarboxylic acids. *Ind. Eng. Chem.* **43**, 2332-2334 (1951).

11 Haszeldine, R. New General Methods for the Synthesis of Fluoroiodides and Fluoroacids. *Nature* **166**, 192-193 (1950).

12 Schulman, F. & Zisman, W. Surface chemical properties of solids coated with a monolayer of perfluorodecanoic acid. *J. Am. Chem. Soc.* **74**, 2123-2124 (1952).

13 D'Agostino, L. A. & Mabury, S. A. Identification of novel fluorinated surfactants in aqueous film forming foams and commercial surfactant concentrates. *Environ. Sci. Technol.* **48**, 121-129 (2014).

14 Barzen-Hanson, K. A. *et al.* Discovery of 40 classes of per-and polyfluoroalkyl substances in historical aqueous film-forming foams (AFFFs) and AFFF-impacted groundwater. *Environ. Sci. Technol.* **51**, 2047-2057 (2017).

15 Begley, T. *et al.* Perfluorochemicals: potential sources of and migration from food packaging. *Food Addit. Contam.* **22**, 1023-1031 (2005).

16 Lang, J. R., Allred, B. M., Peaslee, G. F., Field, J. A. & Barlaz, M. A. Release of per-and polyfluoroalkyl substances (PFASs) from carpet and clothing in model anaerobic landfill reactors. *Environ. Sci. Technol.* **50**, 5024-5032 (2016).

17 Hancock, H. & Cataldi, A. New temperature programming technique for gas chromatography. *J. Chromatogr. Sci.* **5**, 406-408 (1967).

18 Eleuterio, H. Polymerization of perfluoro epoxides. *J. Macromol. Sci., Chem.* **6**, 1027-1052 (1972).

19 Mauritz, K. A. & Moore, R. B. State of understanding of Nafion. *Chem. Rev.* **104**, 4535-4586 (2004).

20 Philips, F. J., Segal, L. & Loeb, L. The application of fluorochemicals to cotton fabrics to obtain oil and water repellent surfaces. *Text. Res. J.* **27**, 369-378 (1957).

21 Downer, A., Eastoe, J., Pitt, A. R., Simister, E. A. & Penfold, J. Effects of hydrophobic chain structure on adsorption of fluorocarbon surfactants with either CF_3- or $H-CF_2-$ terminal groups. *Langmuir* **15**, 7591-7599 (1999).

22 Murray, H. & Milton, B. Terminally branched and terminally monochlorinated perfluorocarboxylic acids. U.S. Patent 3232970A (1966).

23 Barnhart, W., Seffl, R., Wade, R., West, F. & Zollinger, J. Physical and chemical properties of a new series of carboxylic acids, $Cl(CF_2CFCl)_xCF_2CO_2H$. *Ind. Eng. Chem. Chem. Eng. Data Series* **2**, 80-83 (1957).

24 Shi, G. *et al.* Chronic exposure to 6: 2 chlorinated polyfluorinated ether sulfonate acid (F-53B) induced hepatotoxic effects in adult zebrafish and disrupted the PPAR signaling pathway in their offspring. *Environ. Pollut.* **249**, 550-559 (2019).

25 Yao, J. *et al.* Novel perfluoroalkyl ether carboxylic acids (PFECAs) and sulfonic acids (PFESAs): occurrence and association with serum biochemical parameters in residents living near a fluorochemical plant in China. *Environ. Sci. Technol.* **54**, 13389-13398 (2020).

26 Guo, H. *et al.* Exposure to GenX and its novel analogs disrupts hepatic bile acid metabolism in male mice. *Environ. Sci. Technol.* (2021).

27 Ma, D. *et al.* A critical review on transplacental transfer of per-and polyfluoroalkyl substances: prenatal exposure levels, characteristics, and mechanisms. *Environ. Sci. Technol.* (2021).

28 Strynar, M. *et al.* Identification of novel perfluoroalkyl ether carboxylic acids (PFECAs) and sulfonic acids (PFESAs) in natural waters using accurate mass time-of-flight mass spectrometry (TOFMS). *Environ. Sci. Technol.* **49**, 11622-11630 (2015).

29 Sun, M. *et al.* Legacy and emerging perfluoroalkyl substances are important drinking water contaminants in the Cape Fear River Watershed of North Carolina. *Environ. Sci. Technol. Lett.* **3**, 415-419 (2016).
30 McCord, J. & Strynar, M. Identification of per-and polyfluoroalkyl substances in the cape fear river by high resolution mass spectrometry and nontargeted screening. *Environ. Sci. Technol.* **53**, 4717-4727 (2019).
31 Gebbink, W. A., Van Asseldonk, L. & Van Leeuwen, S. P. Presence of emerging per-and polyfluoroalkyl substances (PFASs) in river and drinking water near a fluorochemical production plant in the Netherlands. *Environ. Sci. Technol.* **51**, 11057-11065 (2017).
32 Liu, Y., Pereira, A. D. S. & Martin, J. W. Discovery of C5–C17 poly-and perfluoroalkyl substances in water by in-line SPE-HPLC-Orbitrap with in-source fragmentation flagging. *Anal. Chem.* **87**, 4260-4268 (2015).
33 Newton, S. *et al.* Novel polyfluorinated compounds identified using high resolution mass spectrometry downstream of manufacturing facilities near Decatur, Alabama. *Environ. Sci. Technol.* **51**, 1544-1552 (2017).
34 Awchi, M., Gebbink, W. A., Berendsen, B. J., Benskin, J. P. & van Leeuwen, S. P. Development, validation, and application of a new method for the quantitative determination of monohydrogen-substituted perfluoroalkyl carboxylic acids (H–PFCAs) in surface water. *Chemosphere* **287**, 132143 (2022).
35 Song, X., Vestergren, R., Shi, Y., Huang, J. & Cai, Y. Emissions, transport, and fate of emerging per-and polyfluoroalkyl substances from one of the major fluoropolymer manufacturing facilities in China. *Environ. Sci. Technol.* **52**, 9694-9703 (2018).
36 Wang, Y. *et al.* Suspect and nontarget screening of per-and polyfluoroalkyl substances in wastewater from a fluorochemical manufacturing park. *Environ. Sci. Technol.* **52**, 11007-11016 (2018).
37 Washington, J. W. *et al.* Nontargeted mass-spectral detection of chloroperfluoropolyether carboxylates in New Jersey soils. *Science* **368**, 1103-1107 (2020).
38 Hauptschein, M. & Braid, M. Halogenated organic compounds. U.S. Patent 3002031A (1961).
39 Wang, S. *et al.* First report of a Chinese PFOS alternative overlooked for 30 years: its toxicity, persistence, and presence in the environment. *Environ. Sci. Technol.* **47**, 10163-10170 (2013).
40 Dohany, J. E. Method of preparing high quality vinylidene fluoride polymer in aqueous emulsion. U.S. Patent 4360652A (1982).
41 Perfluoro Sulfonic Acid Group (Shanghai Institute of Organic Chemistry, Academia Sinica). Perfluoro and polyfluoro sulfonic acids--ii. the preparation of some oxapolyfluoroalkane sulfonic acids. *Acta Chim. Sin. (in Chinese)* **37**, 315-324 (1979).
42 Ti, B., Li, L., Liu, J. & Chen, C. Global distribution potential and regional environmental risk of F-53B. *Sci. Total Environ.* **640**, 1365-1371 (2018).
43 Liu, W. *et al.* Atmospheric chlorinated polyfluorinated ether sulfonate and ionic perfluoroalkyl acids in 2006 to 2014 in Dalian, China. *Environ. Toxicol. Chem.* **36**, 2581-2586 (2017).
44 Ruan, T., Lin, Y., Wang, T., Liu, R. & Jiang, G. Identification of novel polyfluorinated ether sulfonates as PFOS alternatives in municipal sewage sludge in China. *Environ. Sci. Technol.* **49**, 6519-6527 (2015).

45 EFSA Panel on Food Contact Materials E Flavourings and Processing Aids (CEF). Scientific opinion on the safety evaluation of the substance perfluoro acetic acid, α-substituted with the copolymer of perfluoro-1, 2-propylene glycol and perfluoro-1, 1-ethylene glycol, terminated with chlorohexafluoropropyloxy groups, CAS No. 329238–24–6 for use in food contact materials. *EFSA J.* **8**, 1519 (2010).
46 Walther, H. C.; Epstein, R. M.; Ferstandig, L. L. *Synthetics, Mineral Oils, and Bio-Based Lubricants* 217-226 (CRC Press, 2020).
47 DelRaso, N., Auten, K., Higman, H. & Leahy, H. Evidence of hepatic conversion of C6 and C8 chlorotrifluoroethylene (CTFE) oligomers to their corresponding CTFE acids. *Toxicol. Lett.* **59**, 41-49 (1991).
48 Huang, L., Dong, W. & Hou, H. Investigation of the reactivity of hydrated electron toward perfluorinated carboxylates by laser flash photolysis. *Chem. Phys. Lett.* **436**, 124-128 (2007).
49 Park, H. *et al.* Reductive defluorination of aqueous perfluorinated alkyl surfactants: effects of ionic headgroup and chain length. *J. Phys. Chem. A* **113**, 690-696 (2009).
50 Song, Z., Tang, H., Wang, N. & Zhu, L. Reductive defluorination of perfluorooctanoic acid by hydrated electrons in a sulfite-mediated UV photochemical system. *J. Hazard. Mater.* **262**, 332-338 (2013).
51 Cui, J., Gao, P. & Deng, Y. Destruction of per-and polyfluoroalkyl substances (PFAS) with advanced reduction processes (ARPs): A critical review. *Environ. Sci. Technol.* **54**, 3752-3766 (2020).
52 Bentel, M. J. *et al.* Defluorination of per-and polyfluoroalkyl substances (PFASs) with hydrated electrons: Structural dependence and implications to PFAS remediation and management. *Environ. Sci. Technol.* **53**, 3718-3728 (2019).
53 Bentel, M. J. *et al.* Enhanced degradation of perfluorocarboxylic acids (PFCAs) by UV/sulfite treatment: Reaction mechanisms and system efficiencies at pH 12. *Environ. Sci. Technol. Lett.* **7**, 351-357 (2020).
54 Bao, Y., Huang, J., Cagnetta, G. & Yu, G. Removal of F–53B as PFOS alternative in chrome plating wastewater by UV/Sulfite reduction. *Water Res.* **163**, 114907 (2019).
55 Gao, J. *et al.* Defluorination of omega-hydroperfluorocarboxylates (ω-HPFCAs): Distinct reactivities from perfluoro and fluorotelomeric carboxylates. *Environ. Sci. Technol.* **55**, 14146–14155 (2021).
56 Liu, Z. *et al.* Near-quantitative defluorination of perfluorinated and fluorotelomer carboxylates and sulfonates with integrated oxidation and reduction. *Environ. Sci. Technol.* **55**, 7052-7062 (2021).
57 Li, X. *et al.* Efficient reductive dechlorination of monochloroacetic acid by sulfite/UV process. *Environ. Sci. Technol.* **46**, 7342-7349 (2012).
58 Seppelt, K. Trifluoromethanol, CF_3OH. *Angew. Chem., Int. Ed. Engl.* **16**, 322-323 (1977).
59 Rao, D. *et al.* New mechanistic insights into the transformation of reactive oxidizing species in an ultraviolet/sulfite system under aerobic conditions: Modeling and the impact of Mn(II). *ACS ES&T Water* **1**, 1785-1795 (2021).
60 Cao, Y., Qiu, W., Li, J., Jiang, J. & Pang, S. Review on UV/sulfite process for water and wastewater treatments in the presence or absence of O_2. *Sci. Total Environ.* **765**, 142762 (2021).

61 Buxton, G. V., Greenstock, C. L., Helman, W. P. & Ross, A. B. Critical review of rate constants for reactions of hydrated electrons, hydrogen atoms and hydroxyl radicals (·OH/·O⁻ in aqueous solution. *J. Phys. Chem. Ref. Data.* **17**, 513-886 (1988).

62 Bentel, M. J. *et al.* Degradation of perfluoroalkyl ether carboxylic acids with hydrated electrons: Structure–reactivity relationships and environmental implications. *Environ. Sci. Technol.* **54**, 2489-2499 (2020).

63 Qian, Y. *et al.* Perfluorooctanoic acid degradation using UV–persulfate process: modeling of the degradation and chlorate formation. *Environ. Sci. Technol.* **50**, 772-781 (2016).

64 Ren, C. *et al.* Catalytic reduction of aqueous chlorate with MoO_x immobilized on Pd/C. *ACS Catal.* **10**, 8201-8211 (2020).

65 Glüge, J. *et al.* An overview of the uses of per-and polyfluoroalkyl substances (PFAS). *Environ. Sci.: Process. Impacts* **22**, 2345-2373 (2020).

66 Yu, X., Ceja-Navarro, J. A. & Wu, X. Sublethal toxicity of fluorine-free firefighting foams in soil invertebrate caenorhabditis elegans. *Environ. Sci. Technol. Lett.* (2022).

67 Crittenden, J. C., Trussell, R. R., Hand, D. W., Howe, K. J. & Tchobanoglous, G. *MWH's water treatment: principles and design* (John Wiley & Sons, 2012).

68 Aberlin, M. E. & Bunton, C. A. Spontaneous hydrolysis of sulfonyl fluorides. *J. Org. Chem.* **35**, 1825-1828 (1970).

69 Tenorio, R. *et al.* Destruction of per-and polyfluoroalkyl substances (PFASs) in aqueous film-forming foam (AFFF) with UV-sulfite photoreductive treatment. *Environ. Sci. Technol.* **54**, 6957-6967 (2020).

70 Wong, G. T. & Zhang, L. Chemical removal of oxygen with sulfite for the polarographic or voltammetric determination of iodate or iodide in seawater. *Mar. Chem.* **38**, 109-116 (1992).

71 Neta, P., Huie, R. E. & Ross, A. B. Rate constants for reactions of inorganic radicals in aqueous solution. *J. Phys. Chem. Ref. Data* **17**, 1027-1284 (1988).

72 Wilson, R. F. Measure of organic carbon in seawater. *Limnol. Oceanogr.* **6**, 259-261 (1961).

73 Menzel, D. W. & Corwin, N. The measurement of total phosphorus in seawater based on the liberation of organically bound fractions by persulfate oxidation. *Limnol. Oceanogr.* **10**, 280-282 (1965).

74 Hosomi, M. & Sudo, R. Simultaneous determination of total nitrogen and total phosphorus in freshwater samples using persulfate digestion. *Int. J. Environ. Stud.* **27**, 267-275 (1986).

75 Liu, J. *et al.* Reductive defluorination of branched per-and polyfluoroalkyl substances with cobalt complex catalysts. *Environ. Sci. Technol. Lett.* **5**, 289-294 (2018).